Drug Design, Development and Therapy Dovepress

Open Access Full Text Article ORIGINAL RESEARCH

Chaihu-Shugan-San Ameliorated Osteoporosis of Mice with Depressive Behavior Caused by Chronic Unpredictable Mild Stress via Repressing Neuroinflammation and HPA Activity

Ming-Chao He[1,2,*], Shi-Hui Xia[2,3,*], Hao Pan[4,*], Ting-Ting Zhou[5], Xin-Luan Wang[6], Ji-Ming Li[6], Xiao-Ming Li[5], Yan Zhang[2,3]

[1]Department of Pain Medicine, The First Affiliated Hospital of Zhengzhou University, Zhengzhou, 450052, People's Republic of China; [2]Spine Disease Research Institute, Longhua Hospital, Shanghai University of Traditional Chinese Medicine, Shanghai, 200032, People's Republic of China; [3]Key Laboratory of Theory and Therapy of Muscles and Bones, Ministry of Education, Shanghai, 200032, People's Republic of China; [4]Department of Neurosurgery, Shuguang Hospital, Shanghai University of Traditional Chinese Medicine, Shanghai, 201203, People's Republic of China; [5]Experimental Research Center, Cangzhou Hospital of Integrated TCM-WM, Cangzhou, 061001, People's Republic of China; [6]Translational Medicine R&D Center, Shenzhen Institute of Advanced Technology, Chinese Academy of Sciences, Shenzhen, 518000, People's Republic of China

*These authors contributed equally to this work

Correspondence: Yan Zhang, Longhua Hospital, affiliated to Shanghai University of Traditional Chinese Medicine, Shanghai, 200032, People's Republic of China, Tel +86 21-64385700, Email medicineyan@aliyun.com; Xiao-Ming Li, Cangzhou Hospital of Integrated TCM-WM, Cangzhou, 061001, People's Republic of China, Tel +86 317-2178055, Email lixiaomingcz@126.com

Objective: Depression and osteoporosis are usually concurrent health problems. This study aimed to explore the development of osteoporosis in depressive mice model and investigate the beneficial effects of the classical herbal formula Chaihu-Shugan-San (CHSG) on the brain and bone.

Methods: CHSG powder was prepared by spray-drying following extraction with water. The fingerprint of CHSG was analyzed using liquid chromatography. The depressive-like model was established by chronic unpredictable mild stress (CUMS) in female mice. The depressive behaviors and trabecular bone properties (measured by micro-CT) were detected at 2, 4, 6, and 8 weeks of CUMS. RT-PCR, immunoblotting and immunofluorescence were applied to measure expression of inflammatory cytokines and morphology of microglias in the hippocampus. Biochemical measurements and histological staining on the adrenal gland were carried out to assess the activity of hypothalamic-pituitary-adrenal (HPA) axis. Histological staining, three-point bending strength, and the expression of regulators involved in bone metabolism were determined.

Results: The treatment with CHSG for 8 weeks could ameliorate depressive behaviors, and down-regulate mRNA expression and tissue content of inflammatory factors IL-1β and IL-6 in hippocampus of CUMS mice. The inhibition of CHSG on neuroinflammation might be attributed to its repression of activity in microglias and NLRP3-triggered inflammation pathway. The serum of rats dramatically alleviated LPS-induced phosphorylation of nuclear NFκB (P65) and IκBα and up-regulation of IL-1β and IL-6 proteins in microglia BV2 cells. CUMS induced over-activity of HPA axis shown by the elevation in serum level of ACTH and corticosterone and in area percentage of zona fasciculata, intriguingly, CHSG reversed those changes in HPA system, ameliorated the reduction in mechanical strength and bone mineral density, and regulated bone metabolism factors of CUMS mice.

Conclusion: The chronic stress-induced depression resulted in bone disorders developing to osteoporosis. Chaihu-Shugan-San exerted beneficial effects on skeletal tissue by ameliorating neuroinflammation and HPA over-activity of mice with depression.

Keywords: Chaihu-Shugan-San, depression, hippocampus, HPA, osteoporosis, stress

Received: 6 August 2024
Accepted: 28 November 2024
Published: 12 December 2024

Graphical Abstract

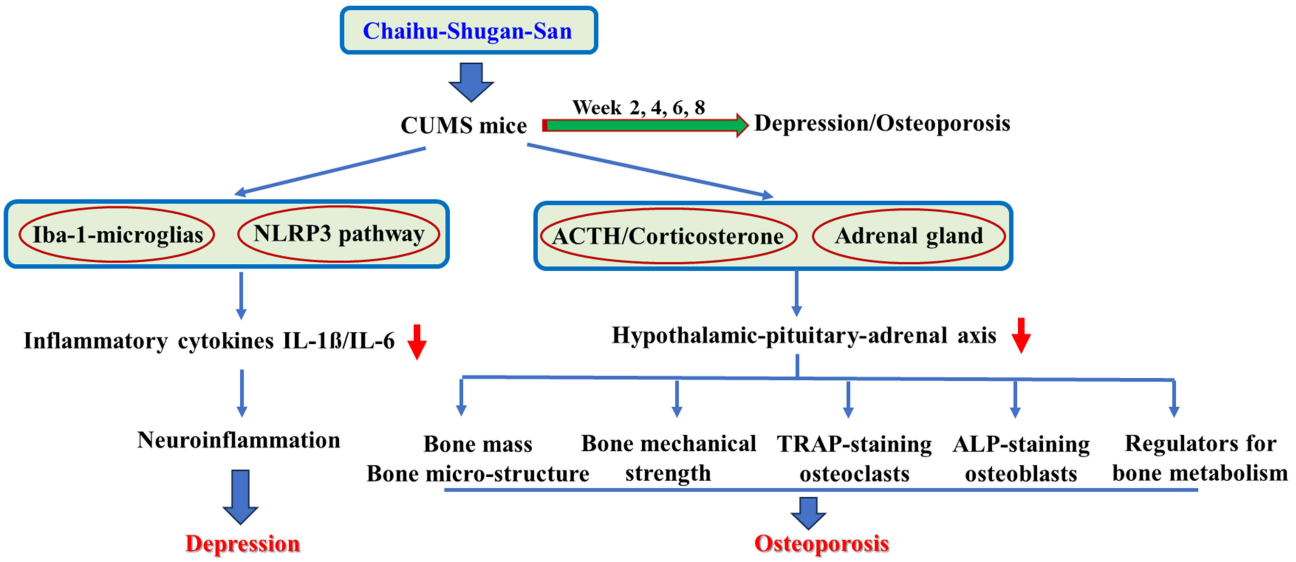

Introduction

An exciting interdependence between two apparently unrelated organs, the bone and the brain, has been reported.[1] A growing body of evidence shows that an injury in central nervous system would result in the progression of metabolic skeletal diseases, such as osteoporosis,[2,3] which is becoming an increasing burden, especially the incident osteoporosis-related fractures, on health care worldwide.[4,5] The neurodegenerative diseases and osteoporosis often coexist, and some studies revealed a causal link, eg, a prospective study from Canada found that cognitive decline was associated with an accelerated rate of bone loss and increased fracture risk in women.[6] Currently, major depression is becoming one of the most prevalent and debilitating personal and public health conditions worldwide.[7] The emerging clinical investigations have figured out that both bone mass (like bone mineral density) and bone quality (like mechanical stiffness) were profoundly decreased in menopause and postmenopausal women with depression in a comparison with those without depression.[8,9] However, the potential underlying mechanism involved in the development of osteoporosis accompanied by depression remains to be clarified.

The endocrine system and the central nervous system, representing major communication systems of the body, are instrumental in the maintenance of whole-organism physiology.[10] In addition to peripheral nervous systems, including sympathetic and parasympathetic nervous systems, it is well illustrated that central neuronal circuitry is tightly interconnected with the pituitary endocrine arm.[11] The glucocorticoids, one of the end hormones of hypothalamic-pituitary-adrenal (HPA) axis, could produce multiple actions on bone metabolism. Both animal and human studies indicated that the chronic psychological stress induced osteoporosis by influencing homeostasis of the HPA axis.[2] We are eager to know if the over-activation of the HPA system participates in the occurrence of depression-related osteoporosis and if there is a therapeutic intervention concurrently preventing depression and osteoporosis and maintaining HPA homeostasis.

The previous studies explicated that the antidepressant drugs could not effectively reduce the risk of osteoporosis,[12] even increasing the risk of bone mass loss.[13] Chaihu-Shugan-San (CHSG), an oriental herbal preparation, is clinically applied in the treatment of chronic gastritis[14] and mastitis,[15] and in improving survival of liver cancer patients.[16] A systematic review demonstrated its therapeutic efficacy in treating post-stroke depression and post-partum depression.[17] One of the purposes of this study is to elucidate whether CHSG could ameliorate stress-induced depressive behavior, especially the main end point of anhedonia, followed by exploring whether CHSG could preserve against osteoporosis associated with depression. Therefore, the animal model established by chronic unpredictable mild stress (CUMS), which is presently the most commonly used, reliable, and effective rodent model of depression,[18] was applied in this study.

The present study first investigated the dynamic changes of depressive behavior and trabecular bone mass and structure of mice during 8-week induction of CUMS. Thereafter, the protective effects of CHSGS against depression and osteoporosis of CUMS mice as well as the potential action mechanism would be dissected.

Materials and Methods

Preparation of Chaihu-Shugan-San

The crude herbs including Bupleuri Radix (240 g), Cyperus rotundus L. (200 g), Chuanxiong Rhizoma (200 g), Citri Reticulatae Pericarpium (240 g), Aurantii Fructus (200 g), Paeoniae Radix Alba (200 g), Glycyrrhizae Radix Et Rhizoma Praeparata Cum Melle (120 g), were purchased from Longhua Hospital (Shanghai University of Traditional Chinese Medicine, China), and identified by the botanist (Prof. Zhou Xin) from the Pharmaceutical Laboratory in Longhua Hospital. A voucher specimen (No. 8032012) for all herbs was deposited in Spine Disease Research Institute (Longhua Hospital). The crude plants were extracted for 1 h after immersing in water (8 folds volume) for 30 min and then filtrated. The residue was extracted again with water (8 folds volume) for 1 h; thereafter, the filtrates were combined and concentrated by rotary evaporation. The powder (387.05 g) of Chaihu-Shugan-San (CHSG), obtained by spray-drying, was applied in further analysis for chemical constitution and in vivo study.

Chromatography for Chaihu-Shugan-San Fingerprint Profiles

About 16.06 mg powder of CHSG was weighed in a 1.5 mL centrifuge tube precisely with 1 mL of methanol. The powder was extracted with ultrasonic for 10 min and filtered with 0.45 μm filter for injection. The CHSG extract (10 μL) was analyzed by Shimazu (Japan) 20AD liquid chromatograph (LC) equipped with Shimazu (Japan) SPD-M40 diode array detector and Agilent (California, USA) reverse chromatography column (Agilent Zorbax Eclipse XDB-C18, 4.6×250 mm, 5 μm). A gradient of water (A: 0.05% formic acid)- acetonitrile (B: 0.05% formic acid) was used as the mobile phase (0–1 min 5% B, 1–5 min 5%–15%B, 15–20 min 20%–30%B, 20–30 min 30%–100%B, 30–35 min 100% B), at a flow rate of 1 mL/min and the column temperature was at 30 °C. The chromatographic peaks were identified by comparing their retention time with those of reference compounds.

Animals and Treatment

The 7-week-old female C57BL/6 mice (n = 60), purchased from Slac Laboratory Animal (Shanghai, China), were housed in environmentally controlled SPF animal facilities, and kept in 22°C with a 12 h light/dark circle and humidity (45–55%)-controlled condition. All animal procedures were performed in accordance with the NIH Guide for Care and Use of Laboratory Animals. The animal study protocol (No. 2019-N013) was reviewed and approved by the Animal Care and Use Committee of Longhua Hospital, affiliated to Shanghai University of Traditional Chinese Medicine. After one-week acclimatization, the mice underwent two rounds of treatments.

In the first round, the mice were randomly allocated into 2 groups. Mice in the normal control group (Control, n = 10) were housed in a separate room with food and water ad libitum, and the depressive model in another group was induced by chronic unpredictable mild stress (CUMS, n = 10) with the following regimens consisting of: food deprivation for 24 h, water deprivation for 24 h, sound exposure by knocking on mice cage for 5 min, placed in wet wood shaving bedding for 24 h, tail clamped for 5 min, shaking for 15 min, restricted in a 50 mL centrifuge tube for 6 h, and crowded in one cage with 10 mice. One of the above eight CUMS operations was selected each day within a week. Food and drinking water were both provided during CUMS except that only water was accessed when food deprivation and only food was accessed when water deprivation. The depressive-like behaviors including tail suspension test (TST) and forced swimming test (FST) and the trabecular bone parameters of mice tibia were measured every 2 weeks.

In the second round, the mice were randomly assigned to four groups including the nonstressed group (Control, n = 10), and the CUMS groups orally treated with vehicle (ddH_2O, 10 mL/kg, n = 10) or low (CHSGL, 1.26 g/kg, n = 10) or high (CHSGH, 3.78 g/kg, n = 10) dose of CHSG by intragastric gavage. The low dose is the clinical equivalent, and the high dose was selected as 3 folds of low dose.

After induction by CUMS for 8 weeks in the above two in vivo experiments, the mice were anesthetized with combined injection (i.p). of ketamine (100 mg/kg) and xylazine (10 mg/kg), hence, serum was collected and stored at −80°C for further biochemical analyses. The bilateral tibias and femurs were aseptically removed and harvested for a variety of analyses as well as the adrenal glands were weighted for calculating tissue index expressed as the average mass of bilateral glands of each mouse divided by body weight.

Depressive Behaviors

The TST, FST, and the sucrose preference test were performed to evaluate depressive-like behaviors of mice. The detection procedure and the corresponding parameters were referred to in the article we previously published.[19]

Biomarkers in Serum and Hippocampus

The tissue levels of cytokine IL-1β and IL-6 in hippocampus were assessed using commercially available enzyme-linked immunosorbent assays (ELISA) kits (Excell, Shanghai, China) according to manufacturer's instructions, and the results were normalized by the protein content of the sample, which in turn was detected using Bradford protein assay (Bio-Rad, CA, USA). The serum level of adrenocorticotropic hormone (ACTH) and corticosterone was determined by ELISA kits (Abcam).

Mechanical Strength of Cortical Bone

Mice femurs underwent a three-point bending mechanical test on a material testing machine (ElectroForce 3200, Bose ElectroForce, MA, USA) to determine maximal force (N, a measure of the maximum force that the bone withstood before fracture) and maximal stress (MPa) as well as elastic modulus (MPa). Each specimen was placed on two supports spaced 3.26 mm apart and the load was applied to the bone midway between the supports at a deformation rate of 0.2 mm/min until fracture occurred. Load–deformation curves were recorded during the bending process.

Micro-Computed Tomography (Micro-CT) Analysis

The tibia of each mouse was fixed in a cylindrical plastic tube to prevent movement of the bone during scanning and scanned with a high-resolution micro vivaCT-80 system (Scanco Medical, Bassersdorf, Switzerland). Trabecular bone was determined by a fixed threshold. After images were captured, 100 slices were established as the volume of interest. The micro-architecture of the trabecular bone at the proximal tibial metaphysis was reconstructed to obtain 3-dimensional (3D) images, and the following quantitative parameters were obtained using μCT Evaluation Program: (1) bone mineral density over total volume (BMD/TV); (2) bone volume over total volume (BV/TV); (3) trabecular bone number (Tb.N).

Histopathological Staining

The separated adrenal glands were fixed in 10% neutral buffered formalin (Wexis, Guangzhou, China) overnight and subsequently embedded in paraffin. Sections were prepared with 5 μm thickness. Hematoxylin and eosin (H&E, Biosharp, Beijing, China) staining was performed for observation and assessment of zona fasciculata. The tibias were fixed, decalcified, and embedded in paraffin by standard histological procedures before serial sections (5 μm) were prepared. Tartrate-resistant acid phosphatase (TRAP) staining (Sigma, St Louis, USA) and alkaline phosphatase (ALP) staining (Yeasen Biotechnology (Shanghai) Co., Ltd., China) were used, respectively, for the identification of osteoclasts and osteoblasts, following the manufacturer's instructions.

Rt-Pcr

Total RNA was extracted from tissues such as hippocampus and femur using TRIzol according to manufacturer's protocol (Invitrogen, Carlsbad, CA, USA). The cDNA synthesis was executed by reverse transcription reactions with 2 μg of total RNA using MMLV reverse transcriptase (Invitrogen, USA) with oligo $dT_{(15)}$ primers (Fermentas). The regular PCR was carried out with cDNAs as the template using a DNA Engine (ABI). β2M served as the housekeeping gene to determine the relative expression of the target genes. The primer sequences used in the present study were included in Table 1.

Table 1 Primer Sequences Used for RT-PCR

Gene	Primer Sequences (5`-3`)	
OPG	Upstream	CTGATGTATGCCCTCAAGCA
	Downstream	AAACAGCCCAGTGACCATTC
RANKL	Upstream	GAAAGGAGGGAGCACGAAAA
	Downstream	TGAAAGCCCCAAAGTACGTC
CAII	Upstream	TGGTTCACTGGAACACCAAA
	Downstream	AGCAAGGGTCGAAGTTAGCA
IL-6	Upstream	CAAGAGACTTCCAGCCAGTTGC
	Downstream	TGTTGTGGGTGGTATCCTCTGTG
IL-1β	Upstream	AATGCCTCGTGCTGTCTGACC
	Downstream	TTGTCGTTGCTTGTCTCTCCTTG
OCN	Upstream	GACACCATGAGGACCATCTTT
	Downstream	TAGAGACCACTCCAGCACA
MMP-9	Upstream	TTAGATCATTCCAGCGTGCC
	Downstream	GCTTAGAGCCACGACCATAC
β2M	Upstream	ACCGGCCTGTATGCTATCCAGAAA
	Downstream	ATTTCAATGTGAGGCGGGTGGAAC

Immunofluorescence and Proportional Area Analysis

Immediately after finishing behavioral tests, mice (n = 6 in each group) were perfused with 4% paraformaldehyde (PFA) and post-fixed overnight before being dehydrated. Ten micrometer coronal sections of the hippocampus were prepared with a Leica CM1950 cryostat microtome (Leica Biosystems, Germany). Sections were rinsed and blocked with 0.3% triton and 5% bovine serum for 1.5h at room temperature, followed by incubation with primary antibodies, which detected Iba-1 (1:200, Abcam) and NeuN (1:200, Abcam) for 24h at 4°C in dark, thereafter incubated with secondary antibodies (Jackson ImmunoResearch, PA, USA) at room temperature for 1h. Images were captured under a microscope (VS120, Olympus, Japan). To quantify the phenotypic changes of microglia, the proportional area with Iba-1 positive staining was analyzed as previously described.[19]

Preparation of Serum of Rats Treated with Chaihu-Shugan-San

The male 8-week-old SD rats purchased from Charles River (Tongxiang, Zhejiang, China) were orally treated with vehicle, low dose (0.87g/kg) of CHSG, and high dose (2.61g/kg) of CHSG by intragastric gavage for 7 consecutive days. After last dosing, the blood was taken from the abdominal aorta, and the serum was prepared for in vitro studies.

Cell Culture and Treatment

Mouse BV2 microglial cells were cultured in DMEM supplemented with 10% FBS containing 100 U/mL penicillin and 100 μg/mL streptomycin at 37°C in a 5% CO_2 humidified incubator. The cells treated with LPS (1 μg/mL) as an inducer for inflammation were incubated with the serum prepared from rats in the absence or presence of NFκB (P65) pathway stimulator prostratin (1 μM) for 12 hours after the cells were seeded onto 6-well plates for 48 hours. The cell protein was isolated by RIPA lysis buffer (Beyotime Biotechnology, China) for immunoblotting on IL-1β and IL-6. The nuclear protein fraction was extracted using the Nuclear Protein Extraction Kit (Beyotime) for immunoblotting on proteins within P65 pathway, including p-IκBα, IκBα, p-P65 and P65.

Western Blotting

The proteins from mice hippocampus were extracted in RIPA lysis buffer containing protease inhibitor cocktails (Roche, Mannheim, Germany). Tissue and cell samples containing 30 μg of protein were separated on SDS-PAGE gel and transferred onto polyvinylidene fluoride (PVDF) membrane. After saturation with 5% (w/v) BSA in TBS and 0.1% (w/v) Tween 20 (TBST), the membranes were incubated with primary antibodies (Iba-1, NLRP3 & IL-6 from Abcam; IL-1β from Santa Cruz; p-IκBα, IκBα, p-P65, P65 & H3 from CST) at dilutions ranging from 1:1000 to 1:2000 at 4°C overnight. After three washes with TBST, membranes were incubated with secondary antibodies and enhanced

chemiluminescence (ECL) solution. Signals were densitometrically assessed by the Lumi-Imager using Lumi-Analyst software (version 3.10, Roche, Mannheim, Germany) and normalized to β-actin (Sigma) to correct for unequal loading.

Statistical Analysis

The data from these experiments were reported as mean ± standard error of mean (SEM) for each group. All statistical analyses were performed using PRISM version 8.0 (GraphPad). Inter-group differences were analyzed by one-way ANOVA, followed by Tukey's multiple comparison test as a post test to compare the group means if overall $P \leq 0.05$. Differences with P values of less than 0.05 were considered statistically significant.

Results

High-Performance Liquid Chromatography Fingerprint of Chaihu-Shugan-San

HPLC analysis (Figure 1A) figured out 8 compounds contained in CHSG extract, including (1) Paeoniflorin, (2) Liquiritin, (3) E-ferulic acid, (4) Naringoside, (5) Hesperidin, (6) Neohesperidin, (7) Glycyrrhizic acid, and (8) Saikosaponin

A

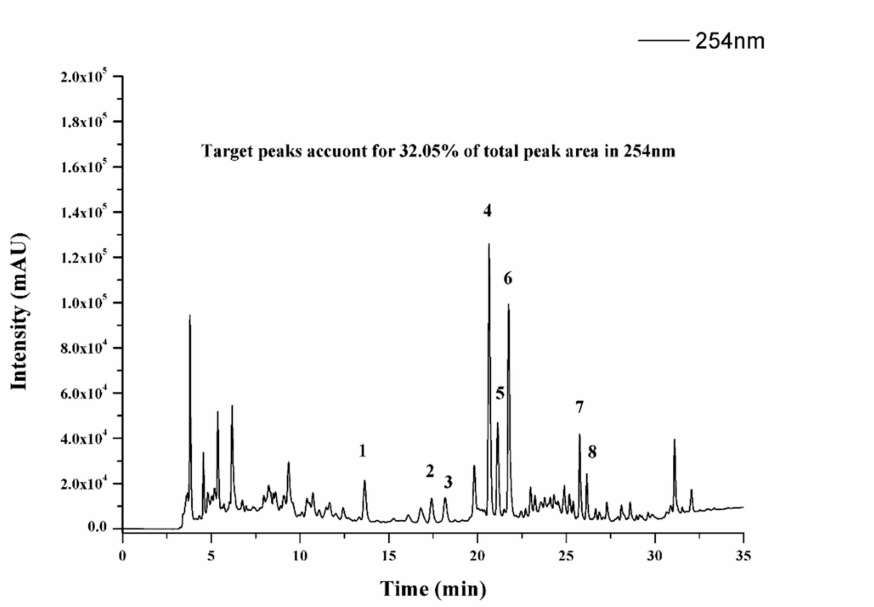

B

Peak No.	Name	RT (min)	Area ratio (%)	Herb sources
1	Paeoniflorin	13.644	2.09	*Paeoniae Radix Alba*
2	Liquiritin	17.405	1.31	*Glycyrrhizae Radix et Rhizoma Praeparata Cum Melle*
3	E-ferulic acid	18.433	1.51	*Chuanxiong Rhizoma*
4	Naringoside	20.709	10.30	*Aurantii Fructus*
5	Hesperidin	21.207	5.02	*Citri Reticulatae Pericarpium*
6	Neohesperidin	21.789	8.50	*Aurantii Fructus*
7	Glycyrrhizic acid	25.725	1.86	*Glycyrrhizae Radix Et Rhizoma Praeparata Cum Melle*
8	Saikosaponin A	26.109	1.46	*Bupleuri Radix*
Total			32.05	

Figure 1 High-performance liquid chromatography (HPLC) analysis for Chaihu-Shugan-San. (**A**) HPLC fingerprint. (**B**) Representative compounds were identified, additionally, the area ratio and the source herbal drug of each compound were presented.

A. The retention time, the percentage of peak area, and the herb source of each compound were presented in Figure 1B. According to Chinese Pharmacopoeia (2020), all of them are the representing components in the constituted herbs. The sum of peak areas of the identified compounds accounted for 32.05% of the total area in HPLC profile of CHSG extract. The amounts of Naringoside and Neohesperidin were the first two highest, which took 10.3% and 8.5% of total area in the whole profile of CHSG powder, respectively.

Depressive-Like Behaviors and Bone Biological Parameters of CUMS Mice

During the period of development of CUMS model, as compared to normal control group, the chronic unpredicted mild stress induced the elevation in immobility time of TST (Figure 2A) and FST (Figure 2B) with statistical difference at week 4 ($P < 0.05$), week 6 ($P < 0.01$), and week 8 ($P < 0.001$); moreover, the difference between control group and

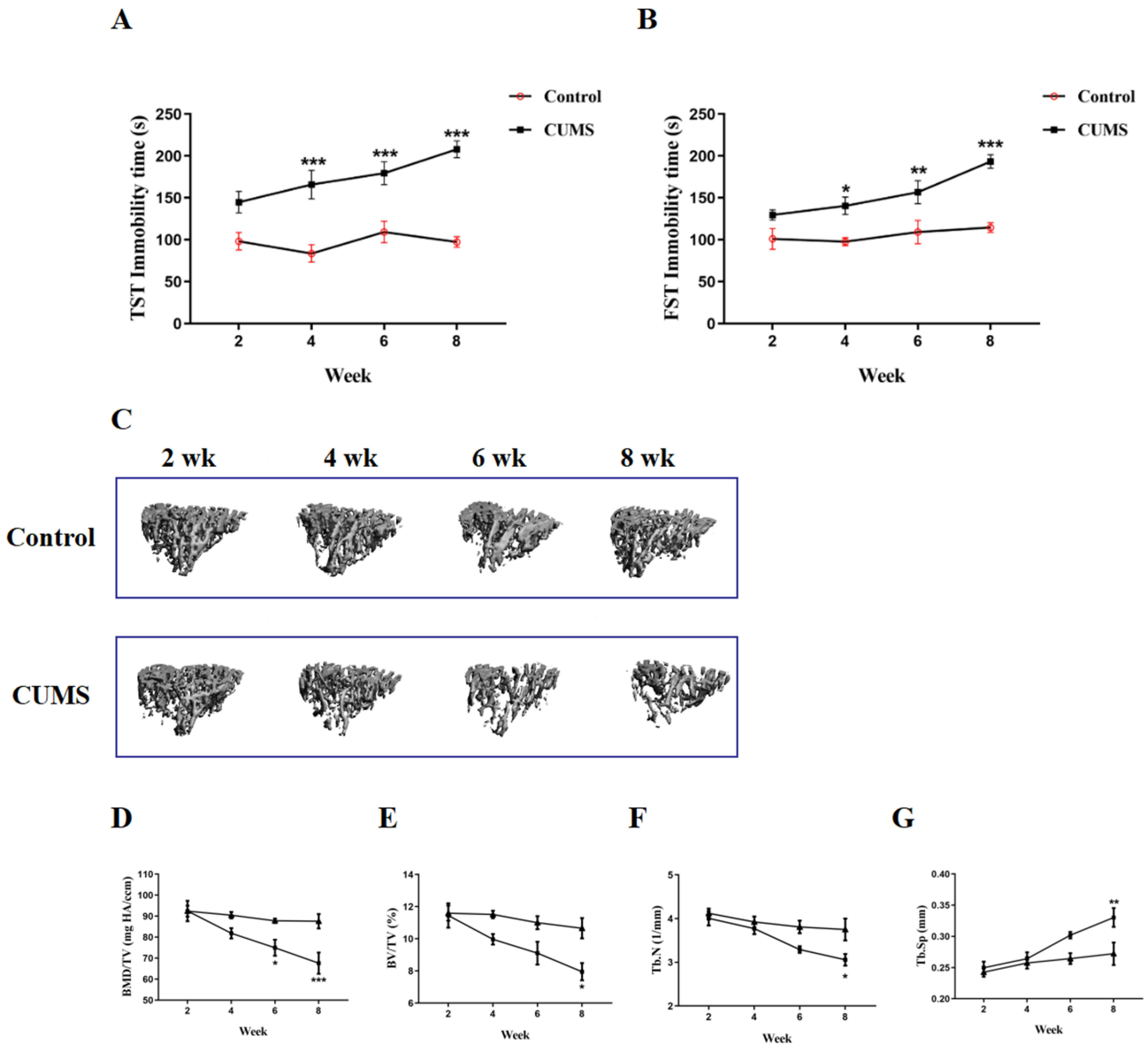

Figure 2 Dynamic changes of depressive behaviors and trabecular bone properties of the mice during the development of chronic unpredictable mild stress (CUMS) for 8 weeks. (**A**) tail suspension test (TST). (**B**) forced swimming test (FST). (**C**) representative images of 3D micro-architecture of the trabecular bone at the proximal tibial metaphysis. The quantitative parameters derived from micro-CT analysis were shown as BMD/TV (**D**), BV/TV (**E**), Tb.N (**F**) and Tb.Sp (**G**). BMD/TV, bone mineral density over total volume; BV/TV, bone volume over total volume; Tb.N, trabecular bone number; Tb.Sp, trabecular bone separation. Values were expressed as mean ± SEM (n = 10). * $P < 0.05$, ** $P < 0.01$, *** $P < 0.001$, vs Control group.

CUMS group was augmented with time changing. When analyzing bone biological parameters from micro-CT detections (Figure 2C), similarly, in a comparison with those in Control group, the CUMS mice exhibited the deteriorations of trabecular bone at proximal tibial metaphysis such as the reduction in bone mineral density (BMD, $P < 0.05$ at week 6 and $P < 0.001$ at week 8, Figure 2D), bone volume over total volume (BV/TV, $P < 0.05$, Figure 2E) and trabecular bone number (Tb.N, $P < 0.05$, Figure 2F) at week 8, and the increase in trabecular bone separation (Tb.Sp, $P < 0.01$, Figure 2G) at week 8.

Chaihu-Shugan-San Ameliorated Behavioral Changes of CUMS Mice

After the administration of CUMS mice with CHSG powder for 8 weeks, the TCM formula treatment significantly ($P < 0.01$) decreased the immobility time in TST (Figure 3A) and FST (Figure 3B) and enhanced the sucrose preference (Figure 3C) in a dose-dependent manner.

Chaihu-Shugan-San Alleviated the Production of Inflammatory Cytokines

Regular PCR analysis (Figure 4A) showed that the treatment with CHSG dramatically ($P < 0.01$) suppressed CUMS-triggered up-regulation in mRNA expression of IL-1β (Figure 4B) and IL-6 (Figure 4C) in hippocampus. Furthermore, the contents of IL-1β (Figure 4D) and IL-6 (Figure 4E) in hippocampus were also lowered ($P < 0.05$) in CUMS mice after 8-week-treatment with CHSG.

Chaihu-Shugan-San Inhibited Neuroinflammation of CUMS Mice

When further clarifying the effects of CHSG on inflammation in the hippocampus, the microglials, one of the main cell populations for the source of inflammation in the central nervous system, and the classical inflammatory pathway were measured. CUMS stimulated the proliferation of microglial cells (green, Figure 5A), especially in the region of NeuN-positive neurons (red, Figure 5A), leading to a large number of microglias distributed among neurons (Iba-1/NeuN, Figure 5A) in hippocampus, which was in accordance with the quantitative data on the proportional area with Iba-1^+ labelling ($P < 0.001$, Figure 5B). Similarly, the immunoblotting analysis (Figure 5D) showed the up-regulation in protein expression of Iba-1 in CUMS group ($P < 0.05$, Figure 5E) as compared to that in Control group.

CHSG treatment lowered the distribution of Iba-1^+ microglias ($P < 0.01$) and downregulated the expression of Iba-1 protein ($P < 0.01$) in hippocampus of mice. Microglias, dynamic cells continuously surveying extracellular environments, would alter morphology as a response to environmental changes. Activated microglia presents an "amoeboid" appearance with repressed processes and enlarged soma as shown in CUMS group in this study (Figure 5C). CHSG treatment obviously reversed the aberrant morphological changes of microglia. Additionally, the treatment with CHSG markedly alleviated CUMS-evoked up-regulation in protein expression of IL-1β ($P < 0.01$, Figure 5F) and NLRP3 ($P < 0.05$, Figure 5G) in hippocampus.

Serum Prepared from Rats Treated with Chaihu-Shugan-San Inhibited NFκB (P65) Pathway in BV2 Cells

Mouse microglial BV2 cells were treated with the inflammatory inducer LPS and the serum prepared from CHSG with the presence or absence of P65 pathway stimulator prostratin. The Giemsa's staining (Figure 6A) showed an amoeboidal morphology with larger and rounder cytoplasm as well as shorter ramification of BV2 cells in response to LPS treatment. The serum containing CHSG improved BV2 cells with oblong cytoplasm and longer pseudopodia, whereas these effects were reversed by the presence of prostratin.

LPS substantially stimulated the phosphorylation of IκBα (Figure 6B and C, $P < 0.05$) and P65 (Figure 6B and D, $P < 0.01$), subsequently resulted in the marked up-regulation of P65 downstream inflammatory protein IL-1ß (Figure 6E and F, $P < 0.01$) and IL-6 (Figure 6E–G, $P < 0.001$). CHSG-containing serum significantly decreased the expression ratio of p-IκBα/IκBα ($P < 0.05$) and p-P65/P65 ($P < 0.05$), and down-regulated protein expression of IL-1ß ($P < 0.05$) and IL-6 ($P < 0.001$) as compared to those of blank serum group in LPS-treated BV2 cells. It was found that the co-treatment with prostratin profoundly blocked the inhibitory effects of the serum prepared from CHSG on p- IκBα/IκBα ($P < 0.05$),

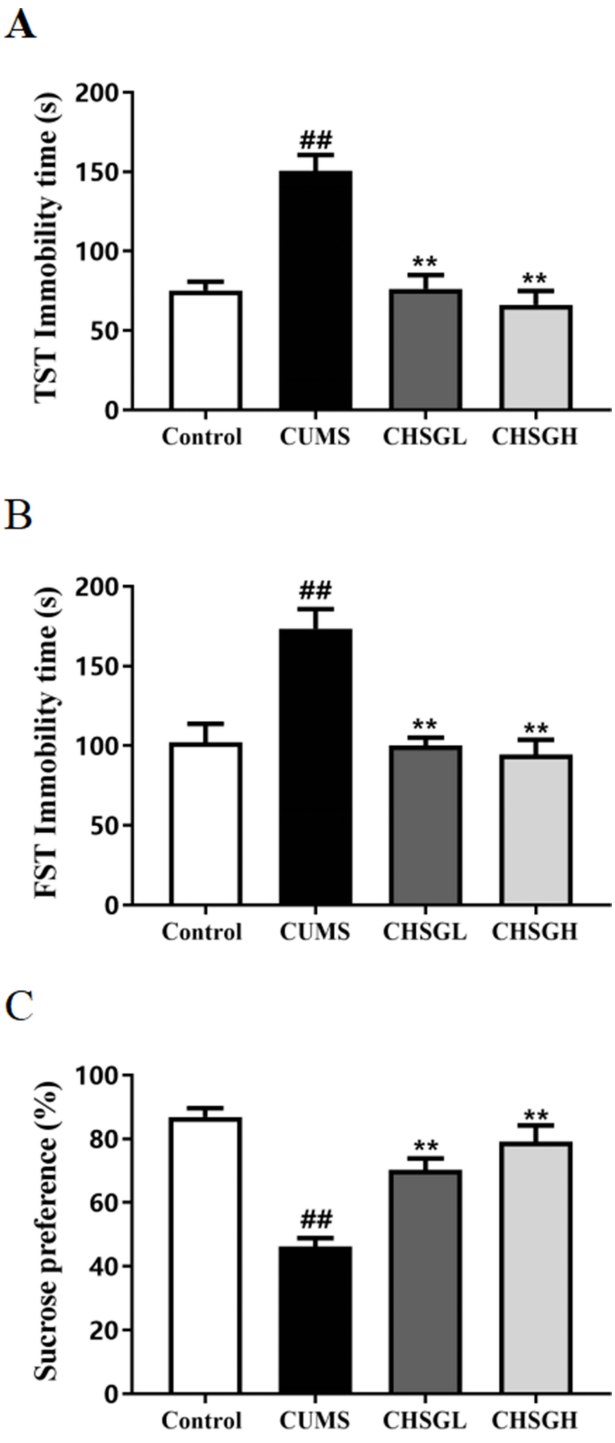

Figure 3 Effects of Chaihu-Shugan-San on depressive behaviors of mice upon to CUMS for 8 weeks. (**A**) tail suspension test (TST). (**B**) forced swimming test (FST). (**C**) sucrose preference. Values were expressed as mean ± SEM (n = 10). ## $P < 0.01$, vs Control group; ** $P < 0.01$, vs CUMS group.

p-P65/P65 ($P < 0.05$), IL-1ß ($P < 0.01$) and IL-6 ($P < 0.05$) in a comparison with the respective CHSG-containing serum group.

Chaihu-Shugan-San Repressed the Activation of HPA Axis of CUMS Mice

The serum contents of ACTH (Figure 7A) and corticosterone (Figure 7B), both of which are vital active components within the HPA axis, were significantly ($P < 0.01$) enhanced in the vehicle-treated CUMS group, and the administration

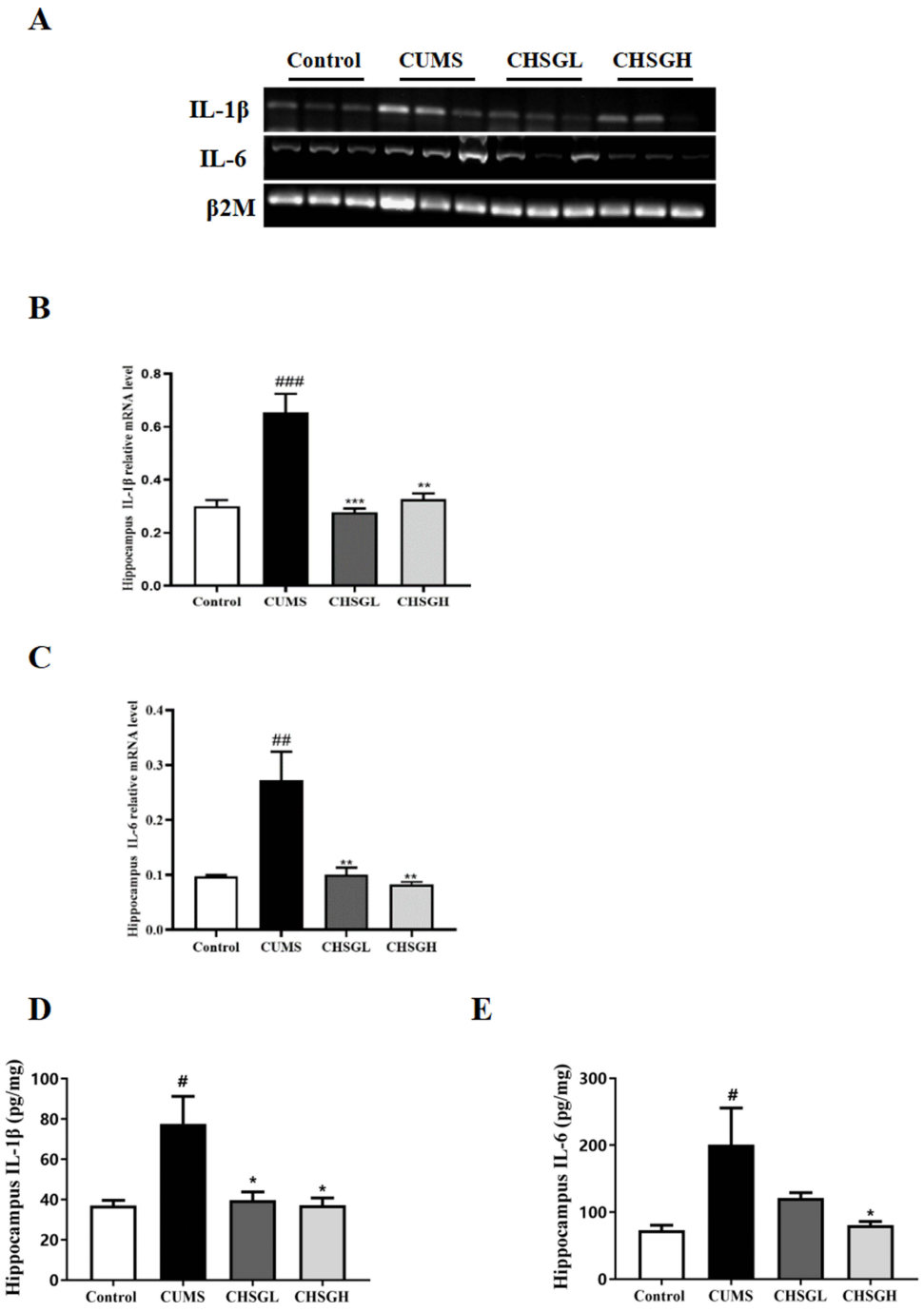

Figure 4 Effects of Chaihu-Shugan-San powder on inflammatory cytokine interleukin-1β (IL-1β) and IL-6 in hippocampus of mice upon to CUMS for 8 weeks. (**A**) RT-PCR detections on mRNA expression of IL-1β and IL-6. (**B** and **C**) the quantitative data on transcriptional level of IL-1β and IL-6, respectively. The contents of IL-1β (**D**) and IL-6 (**E**) were measured in hippocampus of mice. Values were expressed as mean ± SEM (n = 10). # $P < 0.05$, ## $P < 0.01$, ### $P < 0.001$, vs Control group; * $P < 0.05$, ** $P < 0.01$, *** $P < 0.001$, vs CUMS group.

with CHSG at both doses reversed these changes in serum level of ACTH ($P < 0.001$) and corticosterone ($P < 0.05$). The treatment with CHSG dose-dependently inhibited the CUMS-induced rise in adrenal coefficient ($P < 0.01$, Figure 7C); moreover, when identifying the different zones including ZG, ZF, and ZR in adrenal tissue (Figure 7D), the results demonstrated that the area percentage of ZF was much lower in CHSG-treated groups than that in CUMS group ($P < 0.05$, Figure 7E).

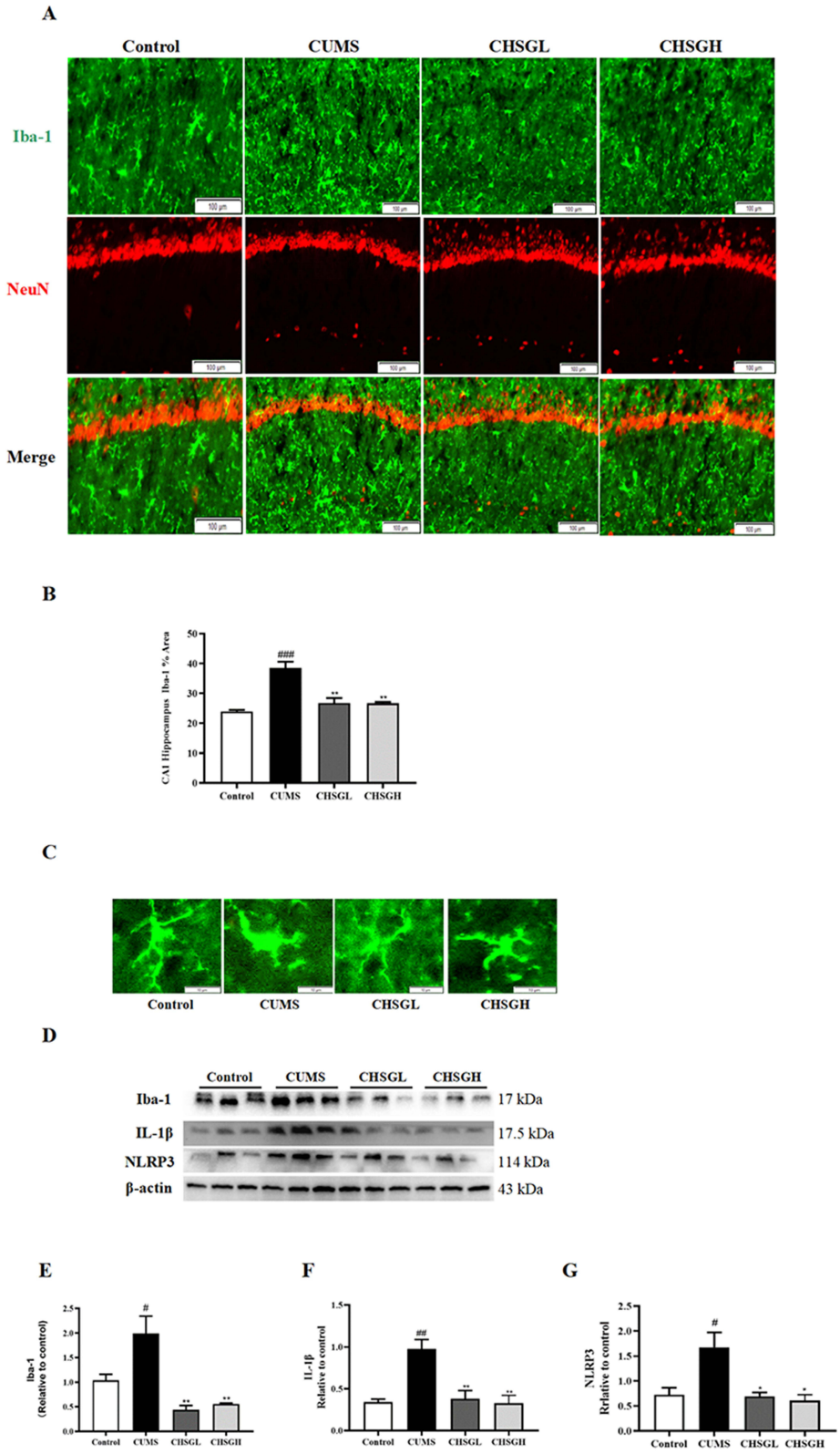

Figure 5 Effects of Chaihu-Shugan-San on specific protein markers of microglias and neurons in hippocampus of mice upon to CUMS for 8 weeks. (**A**), representative images of immunofluorescence staining on Iba-1 (green) and NeuN (red). (**B**) the quantitative data on the proportional area with Iba-1 positive labelling. (**C**) the morphology of microglia stained with microglia-specific anti-Iba-1 antibody. (**D**) immunoblotting on protein expression of Iba-1, IL-1β and NLRP3. (**E–G**), the quantitative data on Western blotting bands. NeuN, neuronal nuclei; Iba-1, ionized calcium binding adaptor molecule-1. Values were expressed as mean ± SEM (n = 10). # $P < 0.05$, ## $P < 0.01$, ### $P < 0.001$, vs Control group; * $P < 0.05$, ** $P < 0.01$, vs CUMS group.

https://doi.org/10.2147/DDDT.S480077 DovePress

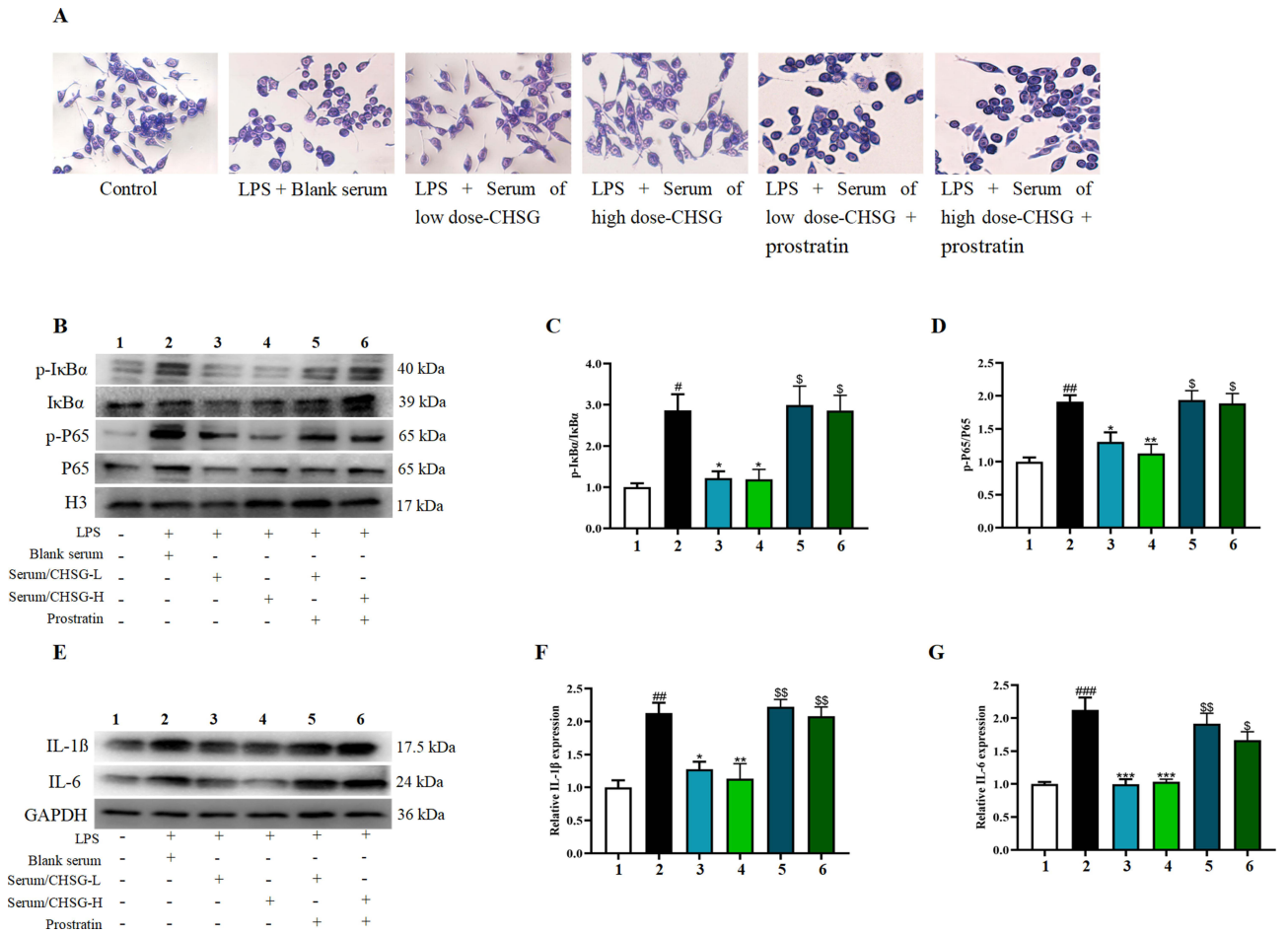

Figure 6 Effects of the serum prepared from rats treated with Chaihu-Shugan-San on NFκB (P65) pathway in BV2 cells. Mouse microglial BV2 cells were treated with LPS and blank serum, or CHSG-containing serum at the absence and the presence of P65 pathway stimulator prostratin. (**A**) Giemsa's staining. (**B** and **E**), immunoblotting bands of nuclear p-IκBα, IκBα, p-P65 & P65, and inflammatory proteins IL-1ß and IL-6. (**C, D, F, G.**), the quantitative data on immunoblotting bands. Values were expressed as mean ± SEM with at least five independent experiments. # $P < 0.05$, ## $P < 0.01$, ### $P < 0.001$, vs normal control; * $P < 0.05$, ** $P < 0.01$, *** $P < 0.001$, vs blank serum group; $ $P < 0.05$, $$ $P < 0.01$, vs the respective CHSG-containing serum group. The indications of the grouping numbers were as the followings, 1, Control; 2, LPS + Blank serum; 3, LPS + Serum of low dose-CHSG; 4, LPS + Serum of high dose-CHSG; 5, LPS + Serum of low dose-CHSG + prostratin; 6, LPS + Serum of high dose-CHSG + prostratin.

Chaihu-Shugan-San Displayed Beneficial Effects on Bone Biological Properties

To investigate if CHSG could protect against bone deteriorations associated with CUMS-induced depression, the mechanical strength of cortical bone (Figure 8A–C) and trabecular bone mass and micro-architecture (Figure 8D–G) were determined. Three-point bending tests demonstrated that CHSG boosted the maximal force ($P < 0.05$, Figure 8A), the maximal stress ($P < 0.05$, Figure 8B), and the elastic modulus ($P < 0.01$, Figure 8C) at the femoral mid-shaft of CUMS mice. Furthermore, the 3D reconstruction (Figure 8G) indicated the protective effects of CHSG on trabecular bone micro-architecture at the proximal metaphysis of CUMS mice tibia. Accordingly, the quantitative data illustrated the preservation of CHSG at high dose on BMD/TV (Figure 8D) and BV/TV (Figure 8E) of CUMS mice ($P < 0.01$), while, no significant effect on Tb.N (Figure 8F).

Chaihu-Shugan-San Exerted Regulatory Effects on the Expression of Factors Associated with Bone Metabolism

In accordance with the destructive effects of CUMS on skeletal systems, the amounts of matured osteoclasts with TRAP-positive staining (Figure 9A) and osteoblasts with ALP-positive staining (Figure 9B) at the proximal tibial metaphysis were markedly increased and decreased, respectively, in CUMS group. The intervention with CHSG for 8 weeks not only

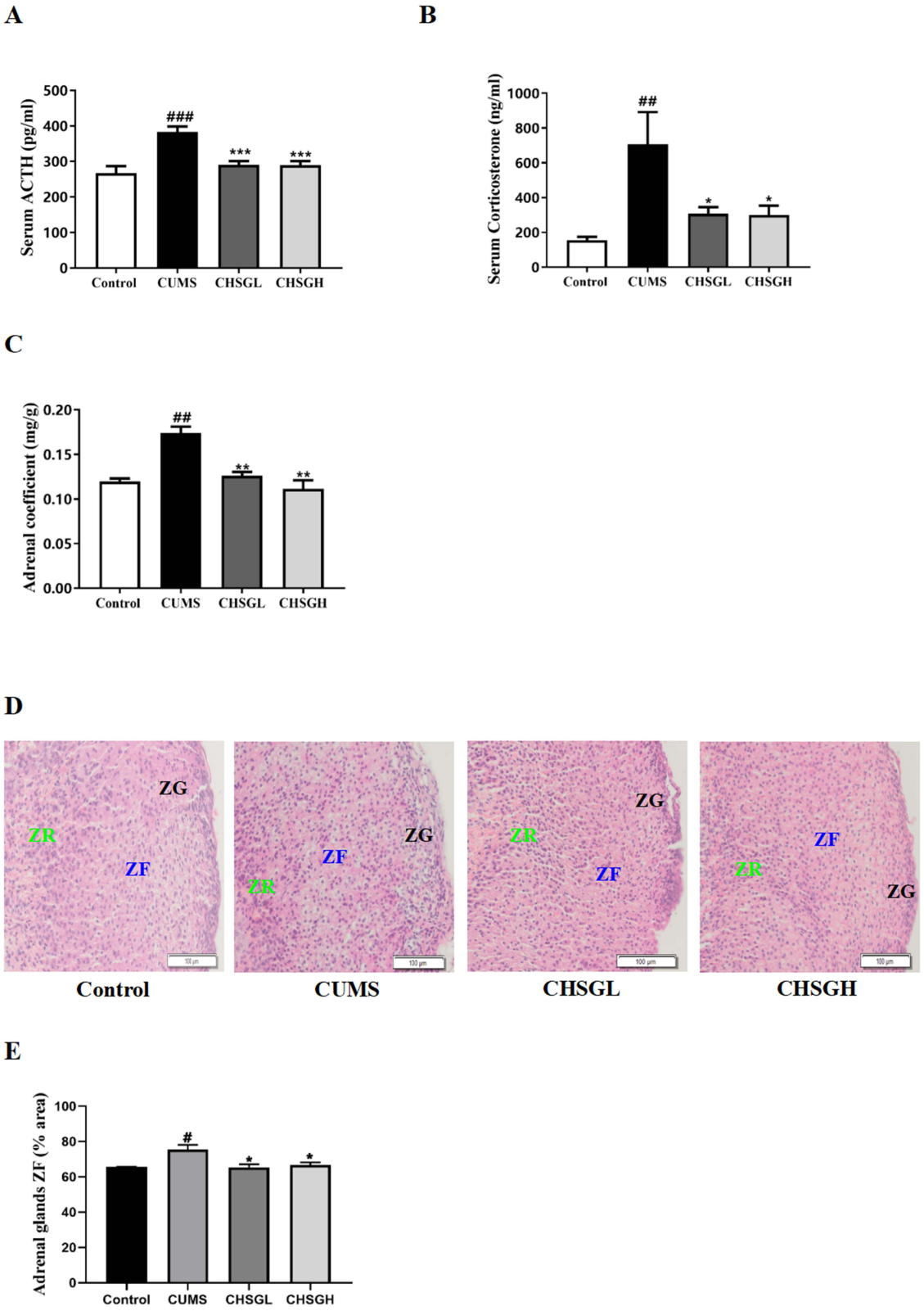

Figure 7 Effects of Chaihu-Shugan-San on hypothalamic-pituitary-adrenal (HPA) axis of mice upon to CUMS for 8 weeks. (**A**) serum ACTH. (**B**) serum corticosterone. (**C**) adrenal index. (**D**) H&E staining on adrenal glands (ZG, ZF and ZR). (**E**) the area ratio of ZF in adrenal glands. Values were expressed as mean ± SEM (n = 10). # $P < 0.05$, ## $P < 0.01$, ### $P < 0.001$, vs Control group; * $P < 0.05$, ** $P < 0.01$, *** $P < 0.001$, vs CUMS group.

Abbreviations: ZR, zona reticularis; ZF, zona fasciculata; ZG, zona glomerulosa.

https://doi.org/10.2147/DDDT.S480077 DovePress

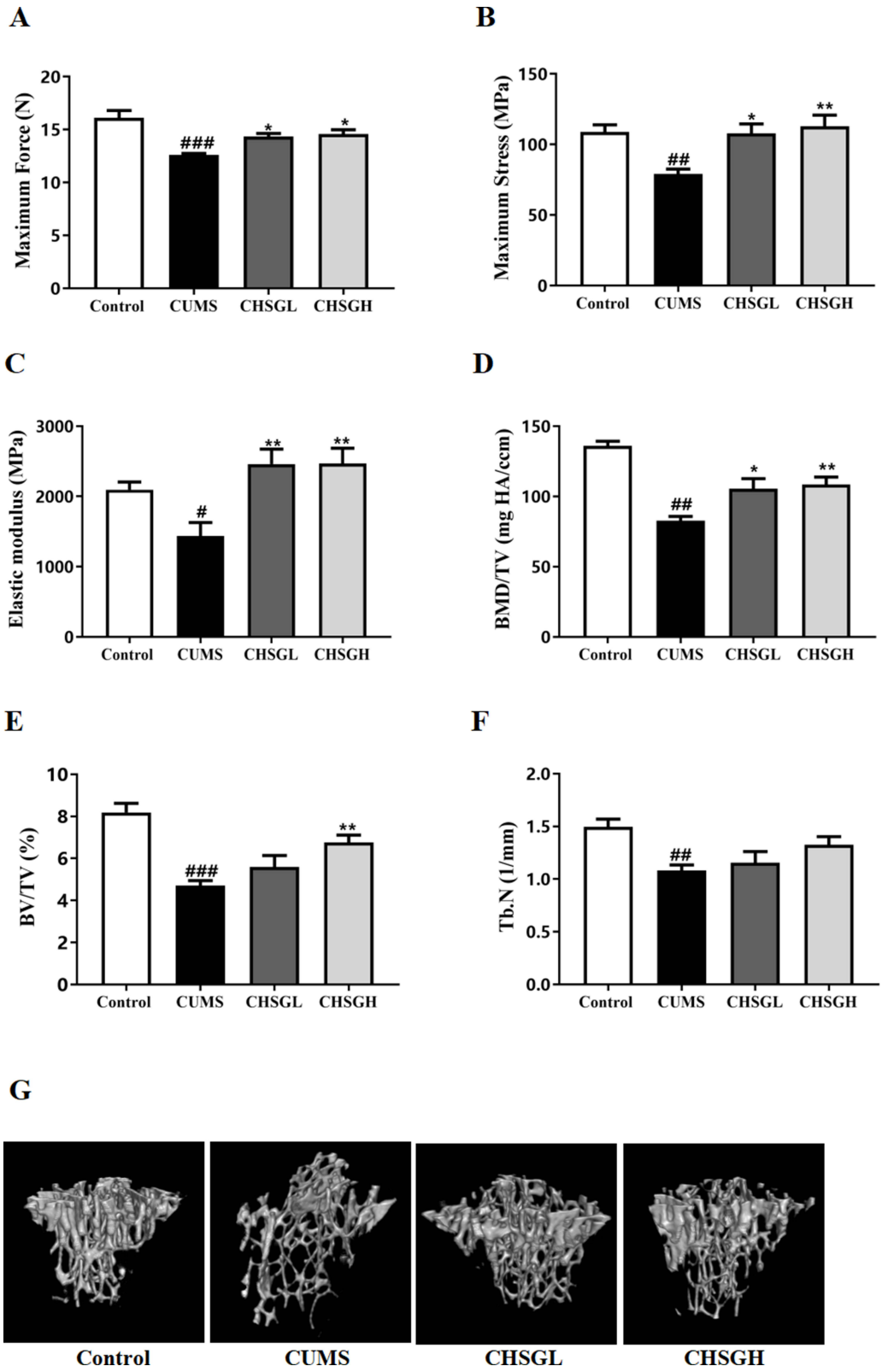

Figure 8 Effects of Chaihu-Shugan-San on biological properties of cortical bone and trabecular bone of mice upon to CUMS for 8 weeks. (**A**–**C**) mechanical strength of cortical bone at mid-shaft of femur. (**D**–**F**) bone mineral density, bone volume and trabecular bone number at proximal tibial metaphysis. (**G**) representative images of 3D micro-structure of trabecular bone. Values were expressed as mean ± SEM (n = 10). # $P < 0.05$, ## $P < 0.01$, ### $P < 0.001$, vs Control group; * $P < 0.05$, ** $P < 0.01$, vs CUMS group.

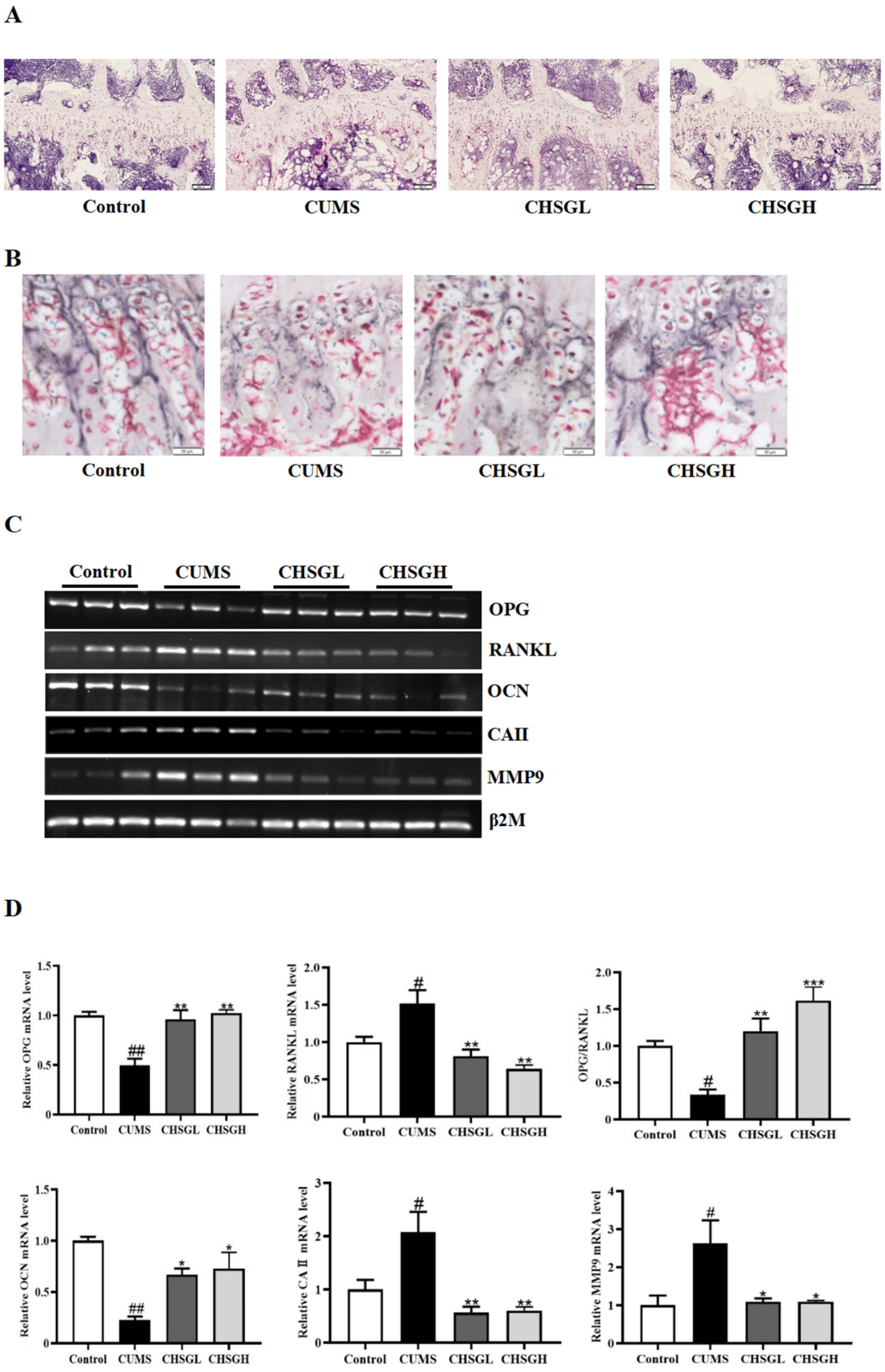

Figure 9 Effects of Chaihu-Shugan-San on factors involved in bone metabolism of mice upon to CUMS for 8 weeks. (**A**) matured osteoclasts at proximal tibial metaphysis by TRAP staining (red-Orange). (**B**) osteoblasts at proximal tibial metaphysis by ALP staining (black purple). (**C**) RT-PCR detections on mRNA expression of OPG, RANKL, OCN, CAII, and MMP9. (**D**) the quantitative data on transcriptional level. Values were expressed as mean ± SEM (n = 10). # $P < 0.05$, ## $P < 0.01$, vs Control group; * $P < 0.05$, ** $P < 0.01$, *** $P < 0.001$, vs CUMS group.

Abbreviations: OPG, osteoprotegerin; RANKL, receptor activator of nuclear factor-κB ligand; OCN, osteocalcin; CAII, carbonic anhydrase II; MMP9, matrix metalloproteinase-9.

reduced the production of matured osteoclasts and enhanced the numbers of osteoblasts but also significantly diminished CUMS-induced up-regulation in mRNA expression of MMP9 ($P < 0.05$), CAII ($P < 0.01$), and RANKL ($P < 0.01$), and down-regulation in mRNA expression of OCN ($P < 0.05$) and OPG ($P < 0.01$), as well as reduction in the expression ratio ($P < 0.01$) of OPG/RANKL (Figure 9C and D).

Discussion

Depression and osteoporosis are severe public health problems.[20] In recent years, osteoporosis has been increasingly identified as a significant comorbidity of major depressive disorder.[21,22] The population-based epidemiological studies have repeatedly shown an increased co-prevalence of fractures and decreased bone mineral density (BMD) accompanied by depression,[22,23] especially in subgroups of women.[9,20,24,25] The present study revealed the occurrence and development of depressive-like behaviors in female mice during the period of 8-week induction by chronic unpredictable mild stress (CUMS). Importantly, in accordance with the clinical observations, the mice displayed the exacerbation of trabecular bone mineral density and micro-structure with the modeling development of CUMS within 8 weeks. Thus, our study preliminarily elucidated that the CUMS model could be applied in future studies on depression-associated osteoporosis, particularly when investigating the interactions among the brain, behavior, and the bone, which newly forms a discipline called "neuropsychosteology".[26]

Conceptually, the mechanisms involved in the affections of depression on bone metabolism could be categorized into biological (like PTH),[8] behavioral, iatrogenic, and comorbidity-related factors.[22] This study tried to clarify the potential pathophysiological pathway underlying this link from the view of biological factors. In addition, the clinical treatments with Western drugs like antipsychotics, valproate, and lamotrigine could not effectively reduce the risk of osteoporosis.[12] However, the antidepressant agents have been proposed to concomitantly combat depression and bone loss,[26] thus, another aim of this study was to clarify the therapeutic efficacy and biological mechanism of traditional herbal formula Chaihu-Shugan-San (CHSG) on depression and osteoporosis in CUMS mice.

In line with previous in vivo rodent studies,[27,28] CHSG could ameliorate depressive-like behaviors of CUMS mice as shown by tail suspension test, forced swimming test, and sucrose preference, supporting the preventive effects of CHSG on stress-induced depression. Emerging evidence illustrates that stress-mediated neuroinflammation destroys brain function and leads to depression-like behaviors, and that the hippocampus is one of the most severely damaged brain regions under stress-induced depression,[29] thereby the inflammation factors in the hippocampus of CUMS mice were detected in this study. Intriguingly, CHSG treatment effectively suppressed the mRNA expression and tissue content of IL-1β and IL-6, both of which are key factors initiating inflammation response in the hippocampus during progression of depression.[30] It is well evident that the dysfunction of different cell types in the brain leads to depression. Microglias, the predominant resident immune cell in the brain, exhibit a critical role in depression by releasing proinflammatory cytokines in response to stress, so it is not hard to understand that recent studies have suggested depression could be regarded as a microglial disease.[31] Administration with CHSG obviously abolished the CUMS-induced high distribution of Iba-1-positive microglial cells among NeuN-staining neural zones in the hippocampus. Moreover, CHSG profoundly repressed the LPS-induced activation of microglial cells as demonstrated by the changes of cell morphology in hippocampus of CUMS mice and in BV2 cells. In addition, the expression of NLRP3 protein, one pivotal component within NLRP3 inflammasome, which is a post-transcriptional regulator for the formation of active form of IL-1β and IL-6,[19,32] was dramatically down-regulated in the hippocampus of CHSG-treated CUMS mice. These results indicated that CHSG could attenuate the stress-evoked depressive-like behaviors via mitigating microglia-involved neuroinflammation.

To further identify the underlying regulatory mechanism of CHSG on microglia-involved neuroinflammation, the mouse BV2 microglial cells were applied in this study. As expected, LPS induced the activation and phosphorylation of nuclear IκBα and P65, which could initiate inflammatory response by stimulating the mRNA transcription of IL-1β and IL-6.[33,34] Importantly, the rats serum containing CHSG exerted suppressive effects on this LPS-evoked pathway by dephosphorylating IκBα and P65, and this regulatory mechanism was strengthened when founding the blocking of P65 pathway stimulator prostratin on the effects of CHSG-containing serum. Thus, the actions of CHSG on NLRP3 pathway and P65 pathway might participate in its repression on neuroinflammation.

Clinically, the dysregulation in the neuroendocrine system, occurring with the neuropsychiatric disorders,[35] might be a high risk of bone disorders, such as the cooccurrence of anxiety and bone loss.[36] The hyperactivity of hypothalamic-pituitary-adrenal (HPA) axis was found in post-stroke depression[37] and melancholic depression.[38] The CUMS-induced depressive mice in this study exhibited the overactivity of HPA axis as shown by the remarkable elevation in serum levels of adrenocorticotropic hormone (ACTH) and corticosterone and in tissue index of adrenal gland as compared to those in non-stressed mice. The treatment with CHSG for 8 weeks resulted in pronounced inhibition of circulating ACTH and corticosterone levels as well as on adrenal hypertrophy of CUMS mice. Based on further histological staining, the area percentage of zona glomerulosa (ZG), zona fasciculata (ZF), and zona reticularis (ZR) were differentiated in adrenal glands, given that these three zones closely correlate with in vivo endocrine functions, in particular, ZF is where the hormone corticosterone formed, which is stimulated by ACTH produced from the anterior pituitary.[39] The CUMS mice showed the hypertrophy of ZF, which is consistent with that the stressful event causes an increase in cortisol production, resulting in the enlargement of the fasciculate zone.[39] Collectively, our study is the first to reveal the inhibitory actions of CHSG on HPA axis hyperactivity triggered by chronic stress.

Large number of studies has uncovered that glucocorticoid-induced osteoporosis, the most common form of secondary osteoporosis, is attributed to the impairment and the promotion of excess glucocorticoids on bone formation and bone resorption, respectively, by interfering with osteoblasts and osteoclasts.[40] Serum levels of endogenous corticosterone of CUMS mice in this study were increased due to the stimulation of HPA cascade signaling, leading to the obvious reductions in mechanical strength of cortical bone and in bone mineral density of trabecular bone, in accordance with an early study where the stressed transgenic mouse model, in which glucocorticoid signaling was selectively disrupted in mature osteoblasts, did not show loss of bone mass.[41] As expected, the regulations of CHSG on the HPA axis could account for its beneficial effects on biological properties of cortical bone and trabecular bone, implicating the feasibility of CHSG in preserving concurrently against the depression and its complication in the skeletal system, osteoporosis.

In an attempt to further confirm the influences of this herbal formula on bone tissue associated with its marked repression on neuroinflammation, depression and HPA axis, the regulators responsible for bone metabolism were evaluated. Our results clearly demonstrated that CUMS stimulated a rise in mRNA expression of genes involved in bone resorption (carbonic anhydrase 2, CAII; matrix metalloproteinase-9, MMP-9) and a drop in mRNA expression of genes involved in bone formation (osteocalcin, OCN), suggesting alterations of bone homeostasis following chronic stress. These data might, at least partially, explain a reduction in BMD and a change in bone turnover of patients with stressful life events.[42]

Treatment of CUMS mice with CHSG promoted the amounts of osteoblasts, as well as ameliorated the changes in mRNA expression of MMP-9, CAII, and OCN, and induced a rise in expression ratio of osteoprotegerin (OPG)/receptor activator for nuclear factor κB ligand (RANKL), both of which are produced and secreted from osteoblasts. Thereafter, the TRAP staining evidently displayed that CHSG mitigated CUMS-evoked aggregation of matured osteoclasts at trabecular bone resulting from a rise in this ratio of OPG/RANKL. Our present data strengthened the early investigations revealing the mediation of CHSG on metabolic network-like bone loss using metabolomic analysis for biochemical changes in the hippocampus and serum of chronic variable stress-induced depressive rats.[43]

Taken together, this study confirmed the antidepressive effects of CHSG by inhibiting neuroinflammation via affecting NLRP3 pathway and P65 pathway. As the biological mechanism is concerned, the hyperactivity of the HPA axis associated with chronic stress-induced depression might, at least partially, contribute to bone loss and osteoporosis. We provided the first evidence that the beneficial effects of CHSG on skeletal tissue of CUMS mice were attributed to its mediation on homeostasis of bone metabolism through alleviating depression and activation of the HPA cascade pathway. The further study would explore if CHSG could produce direct effects on osteoclasts and osteoblasts since many natural compounds possess the bioactivities in promoting osteogenesis and repressing bone resorption.[44,45] Totally, HPA axis could be potentially regarded as one of the targets for intervention strategy preventing depression-associated bone loss, and the concurrent therapeutic efficacy of CHSG for depression and osteoporosis would be explored in further clinical trials.

Acknowledgments

This work was supported in part by the National Key R&D Program from the Ministry of Science and Technology of China (2023YFC3504305), Henan Province Medical Science and Technology Tackling Program Joint Co-Construction Project (LHGJ 20240187), and Scientific and Innovative Action Plan from the Science and Technology Commission of Shanghai Municipality (21400760400).

Disclosure

All authors declare that they have no competing interests.

References

1. Rousseaud A, Moriceau S, Ramos-Brossier M, Oury F. Bone-brain crosstalk and potential associated diseases. *Horm Mol Biol Clin Investig*. 2016;28(2):69–83. doi:10.1515/hmbci-2016-0030
2. Azuma K, Adachi Y, Hayashi H, Kubo KY. Chronic psychological stress as a risk factor of osteoporosis. *J UOEH*. 2015;37(4):245–253. doi:10.7888/juoeh.37.245
3. Otto E, Knapstein PR, Jahn D, et al. Crosstalk of brain and bone-clinical observations and their molecular bases. *Int J Mol Sci*. 2020;21(14):4946. doi:10.3390/ijms21144946
4. Aspray TJ, Hill TR. Osteoporosis and the ageing skeleton. *Subcell Biochem*. 2019;91:453–476. doi:10.1007/978-981-13-3681-2_16
5. Ostovar A, Mousavi A, Sajjadi-Jazi SM, et al. The economic burden of osteoporosis in Iran in 2020. *Osteoporos Int*. 2022;33(11):2337–2346. doi:10.1007/s00198-022-06484-x
6. Bliuc D, Tran T, Adachi JD, et al. Canadian Multicentre Osteoporosis Study (CaMos) Research Group. Cognitive decline is associated with an accelerated rate of bone loss and increased fracture risk in women: a prospective study from the Canadian Multicentre Osteoporosis Study. *J Bone Miner Res*. 2021;36(11):2106–2115. doi:10.1002/jbmr.4402
7. Monroe SM, Harkness KL. Major depression and its recurrences: life course matters. *Annu Rev Clin Psychol*. 2022;18:329–357. doi:10.1146/annurev-clinpsy-072220-021440
8. Atteritano M, Lasco A, Mazzaferro S, et al. Bone mineral density, quantitative ultrasound parameters and bone metabolism in postmenopausal women with depression. *Intern Emerg Med*. 2013;8(6):485–491. doi:10.1007/s11739-011-0628-1
9. Bener A, Saleh NM, Bhugra D. Depressive symptoms and bone mineral density in menopause and postmenopausal women: a still increasing and neglected problem. *J Family Med Prim Care*. 2016;5(1):143–149. doi:10.4103/2249-4863.184640
10. Chamouni A, Schreiweis C, Oury F. Bone, brain & beyond. *Rev Endocr Metab Disord*. 2015;16(2):99–113. doi:10.1007/s11154-015-9312-5
11. Idelevich A, Baron R. Brain to bone: what is the contribution of the brain to skeletal homeostasis? *Bone*. 2018;115:31–42. doi:10.1016/j.bone.2018.05.018
12. Köhler-Forsberg O, Rohde C, Nierenberg AA, Østergaard SD. Association of lithium treatment with the risk of osteoporosis in patients with bipolar disorder. *JAMA Psychiatry*. 2022;79(5):454–463. doi:10.1001/jamapsychiatry.2022.0337
13. Rizzoli R, Cooper C, Reginster JY, et al. Antidepressant medications and osteoporosis. *Bone*. 2012;51(3):606–613. doi:10.1016/j.bone.2012.05.018
14. Qin F, Liu JY, Yuan JH. Chaihu-Shugan-San, an oriental herbal preparation, for the treatment of chronic gastritis: a meta-analysis of randomized controlled trials. *J Ethnopharmacol*. 2013;146(2):433–439. doi:10.1016/j.jep.2013.01.029
15. Chou SH, Huang CC, Lin CH, Wu KC, Chiang PJ. General use of Chinese herbal products among female patients with mastitis in Taiwan. *Evid Based Complement Alternat Med*. 2022;3876240. doi:10.1155/2022/3876240
16. Liao YH, Lin CC, Lai HC, Chiang JH, Lin JG, Li TC. Adjunctive traditional Chinese medicine therapy improves survival of liver cancer patients. *Liver Int*. 2015;35(12):2595–2602. doi:10.1111/liv.12847
17. Sun Y, Xu X, Zhang J, Chen Y. Treatment of depression with Chai Hu Shu Gan San: a systematic review and meta-analysis of 42 randomized controlled trials. *BMC Complement Altern Med*. 2018;18(1):66. doi:10.1186/s12906-018-2130-z
18. Antoniuk S, Bijata M, Ponimaskin E, Wlodarczyk J. Chronic unpredictable mild stress for modeling depression in rodents: meta-analysis of model reliability. *Neurosci Biobehav Rev*. 2019;99:101–116. doi:10.1016/j.neubiorev.2018.12.002
19. Feng R, He MC, Li Q, et al. Phenol glycosides extract of Fructus Ligustri Lucidi attenuated depressive-like behaviors by suppressing neuroinflammation in hypothalamus of mice. *Phyto Res*. 2020;34(12):3273–3286. doi:10.1002/ptr.6777
20. Skowrońska-Jóźwiak E, Gałecki P, Głowacka E, Wojtyła C, Biliński P, Lewiński A. Bone metabolism in patients treated for depression. *Int J Environ Res Public Health*. 2020;17(13):4756. doi:10.3390/ijerph17134756
21. Gao H, Huang C, Zhao K, et al. Research progress on the molecular mechanism by which depression affects bone metabolism. *DNA Cell Biol*. 2020;39(5):738–746. doi:10.1089/dna.2019.5284
22. Rosenblat JD, Gregory JM, Carvalho AF, McIntyre RS. Depression and disturbed bone metabolism: a narrative review of the epidemiological findings and postulated mechanisms. *Curr Mol Med*. 2016;16(2):165–178. doi:10.2174/1566524016666160126144303
23. Ma M, Liu X, Jia G, et al. The association between depression and bone metabolism: a US nationally representative cross-sectional study. *Arch Osteoporos*. 2022;17(1):113. doi:10.1007/s11657-022-01154-1
24. Bab IA, Yirmiya R. Depression and bone mass. *Ann N Y Acad Sci*. 2010;1192:170–175. doi:10.1111/j.1749-6632.2009.05218.x
25. Petronijević M, Petronijević N, Ivković M, et al. Low bone mineral density and high bone metabolism turnover in premenopausal women with unipolar depression. *Bone*. 2008;42(3):582–590. doi:10.1016/j.bone.2007.11.010
26. Yirmiya R, Goshen I, Bajayo A, et al. Depression induces bone loss through stimulation of the sympathetic nervous system. *Proc Natl Acad Sci U S A*. 2006;103(45):16876–16881. doi:10.1073/pnas.0604234103
27. Li YH, Zhang CH, Wang SE, Qiu J, Hu SY, Xiao GL. Effects of Chaihu Shugan San on behavior and plasma levels of corticotropin releasing hormone and adrenocorticotropic hormone of rats with chronic mild unpredictable stress depression. *J Chi Inter Med*. 2009;7:1073–1077. doi:10.3736/jcim20091110

28. Teng HY, Xiao JP, Fu YZ, Shi XF. Study on antidepressant effect of Chaihu Shugan Powder in depression model rats with chronic unpredictable mild stress. *Fujian J TCM*. 2022;53(12):19–22. doi:10.13260/j.cnki.jfjtcm.012621
29. Wu Z, Xiao L, Wang H, Wang G. Neurogenic hypothesis of positive psychology in stress-induced depression: adult hippocampal neurogenesis, neuroinflammation, and stress resilience. *Int Immunopharmacol*. 2021;97:107653. doi:10.1016/j.intimp.2021.107653
30. Guo LT, Wang SQ, Su J, et al. Baicalin ameliorates neuroinflammation-induced depressive-like behavior through inhibition of toll-like receptor 4 expression via the PI3K/AKT/FoxO1 pathway. *J Neuroinflammation*. 2019;16(1):95. doi:10.1186/s12974-019-1474-8
31. Wang H, He Y, Sun Z, et al. Microglia in depression: an overview of microglia in the pathogenesis and treatment of depression. *J Neuroinflammation*. 2022;19(1):132. doi:10.1186/s12974-022-02492-0
32. Chen L, Wang H, Ge S, Tai S. IL-6/STAT3 pathway is involved in the regulation of autophagy in chronic non-bacterial prostatitis cells, and may be affected by the NLRP3 inflammasome. *Ultrastruct Pathol*. 2021;45(4–5):297–306. doi:10.1080/01913123.2021.1966149
33. Zheng J, Fan R, Wu H, et al. Directed self-assembly of herbal small molecules into sustained release hydrogels for treating neural inflammation. *Nat Commun*. 2019;10(1):1604. doi:10.1038/s41467-019-09601-3
34. He MC, Shi Z, Qin M, et al. Muscone ameliorates LPS-induced depressive-like behaviors and inhibits neuroinflammation in prefrontal cortex of mice. *Am J Chin Med*. 2020;48(3):559–577. doi:10.1142/S0192415X20500287
35. Ge T, Yao X, Zhao H, et al. Gut microbiota and neuropsychiatric disorders: implications for neuroendocrine-immune regulation. *Pharmacol Res*. 2021;173:105909. doi:10.1016/j.phrs.2021.105909
36. Yang F, Liu Y, Chen S, et al. A GABAergic neural circuit in the ventromedial hypothalamus mediates chronic stress-induced bone loss. *J Clin Invest*. 2020;130(12):6539–6554. doi:10.1172/JCI136105
37. Zhou L, Wang T, Yu Y, et al. The etiology of poststroke-depression: a hypothesis involving HPA axis. *Biomed Pharmacother*. 2022;151:113146. doi:10.1016/j.biopha.2022.113146
38. Juruena MF, Bocharova M, Agustini B, Young AH. Atypical depression and non-atypical depression: is HPA axis function a biomarker? A systematic review. *J Affect Disord*. 2018;233:45–67. doi:10.1016/j.jad.2017.09.052
39. Soetantyo GI, Sarto M. The antidepressant effect of Chlorella vulgaris on female Wistar rats (Rattus norvegicus Berkenhout, 1769) with chronic unpredictable mild stress treatment. *J Tropical Biodiversi Biotechgy*. 2019;4:72–81. doi:10.22146/jtbb.43967
40. Komori T. Glucocorticoid signaling and bone biology. *Horm Metab Res*. 2016;48(11):755–763. doi:10.1055/s-0042-110571
41. Henneicke H, Li J, Kim S, Gasparini SJ, Seibel MJ, Zhou H. Chronic mild stress causes bone loss via an osteoblast-specific glucocorticoid-dependent mechanism. *Endocrinology*. 2017;158(6):1939–1950. doi:10.1210/en.2016-1658
42. Wuertz-Kozak K, Roszkowski M, Cambria E, et al. Effects of early life stress on bone homeostasis in mice and humans. *Int J Mol Sci*. 2020;21(18):6634. doi:10.3390/ijms21186634
43. Su ZH, Jia HM, Zhang HW, Feng YF, An L, Zou ZM. Hippocampus and serum metabolomic studies to explore the regulation of Chaihu-Shu-Gan-San on metabolic network disturbances of rats exposed to chronic variable stress. *Mol Biosyst*. 2014;10(3):549–561. doi:10.1039/c3mb70377k
44. Wang T, Liu Q, Tjhioe W, et al. Therapeutic potential and outlook of alternative medicine for osteoporosis. *Curr Drug Targets*. 2017;18(9):1051–1068. doi:10.2174/1389450118666170321105425
45. He J, Li X, Wang Z, et al. Therapeutic anabolic and anticatabolic benefits of natural Chinese medicines for the treatment of osteoporosis. *Front Pharmacol*. 2019;10:1344. doi:10.3389/fphar.2019.01344